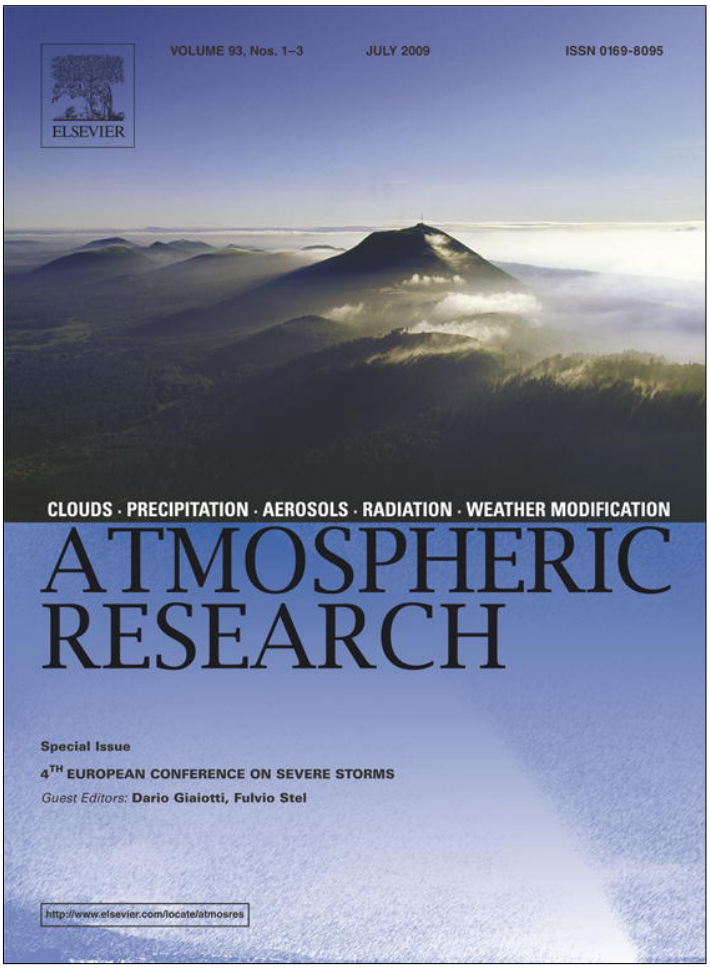

Atmospheric Research 93 (2009) 147–160

Contents lists available at ScienceDirect

Atmospheric Research

journal homepage: www.elsevier.com/locate/atmos

Synoptic and mesoscale diagnosis of a tornado event in Castellcir, Catalonia, on 18th October 2006

Montserrat Aran [a,*], Jéssica Amaro [a], Joan Arús [b], Joan Bech [a], Francesc Figuerola [a], Miquel Gayà [c], Eliseu Vilaclara [a]

[a] Servei Meteorològic de Catalunya, Berlín 38, Barcelona E-08029, Spain
[b] Agencia Estatal de Meteorología, Delegació a Catalunya, Barcelona, Spain
[c] Agencia Estatal de Meteorología, Delegació a les Illes Balears, Palma de Mallorca, Spain

ARTICLE INFO

Article history:
Received 3 December 2007
Received in revised form 26 August 2008
Accepted 28 September 2008

Keywords:
Tornado
Squall line
Bow echo
Catalonia

ABSTRACT

This paper presents a synoptic and mesoscale analysis of a tornadic event in Castellcir, north of Barcelona (Spain), on 18th October 2006. The tornado caused F2 damage but, fortunately, there were no injuries. No strong forcing for upward vertical motion was identified from the synoptic analysis, but conditions were suitable for the development of convection. Despite the fact that CAPE values were not very high (more than 800 J/kg at 12 UTC), the level of free convection was low enough to favour the vertical development. A pivotal factor was the presence of an easterly low level jet and the shear profile of the hodograph near surface. Also, a thermal boundary was detected using surface observations. Operational radar observations allowed defining the precipitating structure as a mesoscale convective system (MCS) but no clear meso-cyclone was found linked to supercells features. The analysis of lightning data suggested three stages of the MCS, and similar results were obtained from the IR images study. Moreover, at the last stage of the MCS a bow echo which caused a microburst was detected at the northeast of Catalonia.

1. Introduction

Catalonia, situated in the northeast of the Iberian Peninsula, is usually affected by significant convective weather events, especially heavy rainfall and subsequent flash floods (Barrera et al., 2006). Although few records of tornadoes exist, these events are also quite frequent in Catalonia. A climatology presented by Gayà (2005) for the period 1987–2005 revealed Catalonia as one of the Spanish regions with the highest density of tornadoes, after the Balearic Islands. Some studies have been carried out by other authors in those areas (see for example Gayà et al., 2001; Homar et al., 2001, 2003; Bech et al., 2007a).

On 18th October 2006, at 11 UTC a cluster of storms grew in the south of Catalonia and crossed it. It was not until 2 h later that a squall line developed. At 13:30 UTC, a tornado was reported in the village of Castellcir (about 50 km north of Barcelona, see Fig. 1). The site survey indicated a track about 4 km in length, oriented from SW to NE, and a maximum width of 260 m. The tornado was rated as F2 in the Fujita Scale (Fujita, 1981) but no significant property damage and injuries were recorded, as it took place in a forest area (Bech et al., 2007b). Many pines, oaks and holm oaks were overturned and some of them were uprooted or snapped, but only a few tiles from nearby houses were removed. After the tornado, a microburst caused some damage in farms and greenhouses in Cabanes, further to the northeast (Fig. 1).

The aim of this study is to characterize this event in order to identify synoptic ingredients and mesoscale factors. This information may help to forecast similar future events. The paper is organised as follows: Section 2 analyses the synoptic frame, Section 3 presents observational data collected by automatic weather stations and from the rawinsonde, Section 4 provides a description of the mesoscale situation using remote sensing observations as satellite, radar and lightning detection network, and conclusions are given in Section 5.

* Corresponding author. Meteorological Service of Catalonia, Berlin 38, Barcelona E-08029, Spain. Tel.: +34 93 567 60 90; fax: +34 93 567 61 02.
E-mail address: maran@meteo.cat (M. Aran).

0169-8095/$ – see front matter © 2008 Elsevier B.V. All rights reserved.
doi:10.1016/j.atmosres.2008.09.031

2. Synoptic scale analysis

The synoptic environment in this event was similar to other cases studied (Homar et al., 2001, 2003; Mateo et al., 2009). A strong baroclinic area was situated over the Atlantic Ocean close to northwest of the Iberian Peninsula. At high levels, there was a negative tilted ridge in the Balearic Islands, and a slight diffluence over Catalonia (Fig. 2 and 3a–b). Synoptic forcing was weak in the area of study compared to the western of the Iberian Peninsula. Martín et al. (1997) also documented a tornadic event in central Spain with weak synoptic forcing conditions.

At mid and low levels, a thermal ridge was centred over the Western Mediterranean area as it can be seen at 850 hPa (Fig. 3c–d). At the mean sea level pressure, the centre of a low was over northwest Spain, and only relative low pressure appeared between Catalonia and the Balearic Islands. Thus, moist and relatively warmer air was impinged by easterly winds over the southern of the Catalonia coast.

At 12 UTC, the airmass in Barcelona presented potential instability as equivalent potential temperature decreased with height until 600 hPa (Fig. 4). Another ingredient for deep, moist convection is CAPE. In this event, it was not too high over the area of study: more than 800 J/kg in Barcelona area and null in the inner part of Catalonia (Fig. 5a–b). The maximum of CAPE was situated over the Mediterranean Sea in the Balearic Islands. However, no convective development was detected in that area (Fig. 10 and 11), as a strong inversion inhibited convection.

Storm relative helicity (srH) is a very useful variable to detect supercell environments (Davies and Johns, 1993; Edwards and Thompson, 2000). Over Catalonia there were moderate values of srH (0–3 km), between 150 and 350 m^2/s^2 (Fig. 5c–d).

Although the synoptic forcing was low over the area of study, the potential instability and the wind shear presented at low levels (1000–850 hPa) were enough to develop strong and organized convection.

3. Observational data

3.1. Automatic weather stations data

From the earliest hours of the day moderate easterly winds blew over Catalonia; the strongest gusts inland were from this direction (Fig. 6b). By midday, deep convection was important and thunderstorms evolved into a squall line structure moving from SW to NE. After the passage of the squall line, the wind veered from east to southwest. This can be appreciated in Fig. 6a which shows the temporal evolution of the wind direction and the speed recorded at the Barcelona Fabra Observatory (altitude: 411 m). The gusts of winds west of Castellcir were recorded between 13:00 and 13:30 UTC (Fig. 6b) and were mainly from southwest direction. As a result, the interaction of the gust front with the main easterly wind favoured the development of a convergence zone. The lack of nearby surface observational data did not allow determining precisely the local triggering mechanism. This was probably influenced by the complex topography of the area as other authors have found examining heavy rainfall events in Catalonia (Campins et al., 2007, Pascual and Callado 2002).

The most remarkable precipitation intensities were recorded in the northern and eastern parts of Catalonia. This last area was affected by the squall line. The maximum rainfall intensity was 23.4 mm in 30 min in Òdena (Fig. 1), with an extreme pulse of 2.6 mm in 1 min at 13:05 UTC.

The air was close to saturation almost everywhere; values of relative humidity were higher than 90% except in the southwest (Fig. 7a). At the eastern part of this area, cells started their development evolving into the squall line. After the most intense precipitation, the temperature only dropped 2 °C, locally 3 °C.

In this tornado event, some amount of horizontal vorticity could be produced in the thermal boundary due to the cooling effect of the anvil (Markowski et al., 1998). At 14 UTC, the hourly total solar radiation, presented in Fig. 7b, shows the area where

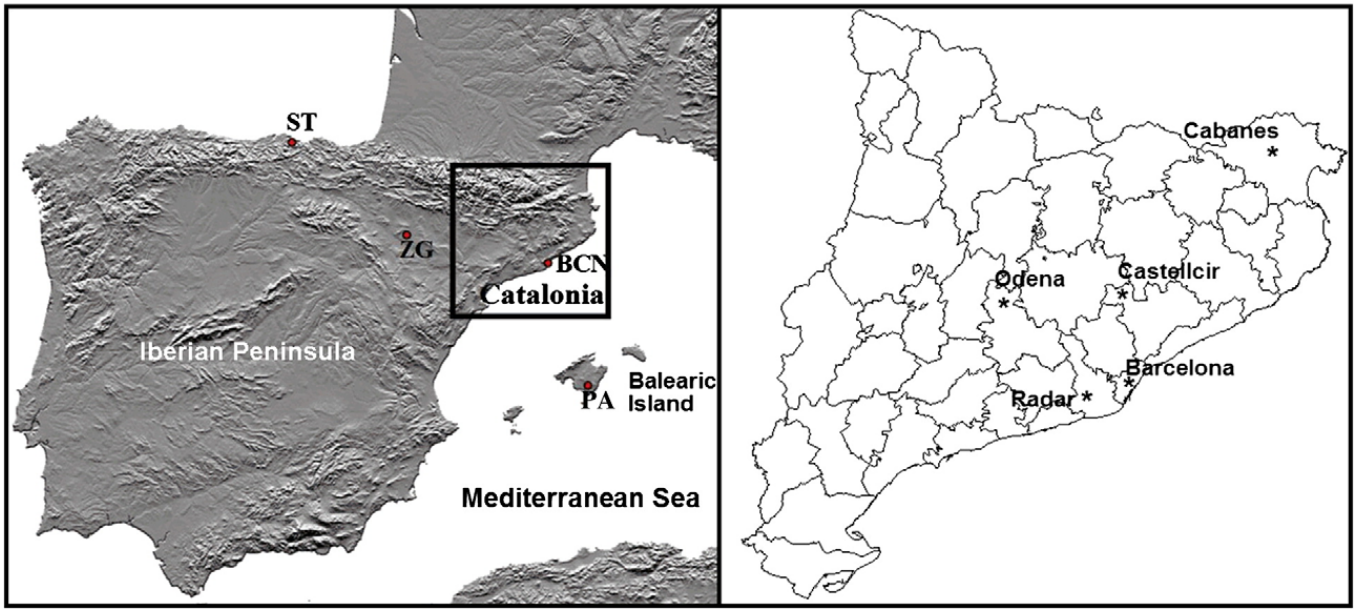

Fig. 1. (a) The Iberian Peninsula and The Balearic Island. (b) a zoom of the area of interest, Catalonia.

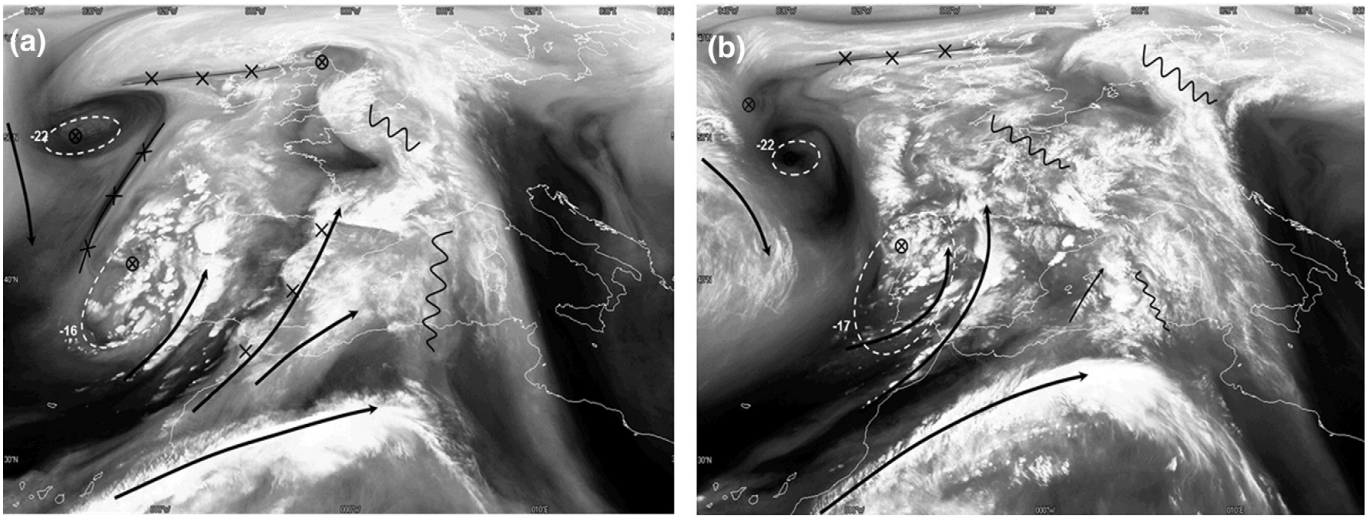

Fig. 2. Water vapour image and subjective reanalysis (a) at 00 UTC and (b) at 12 UTC. Features shown are: maximum wind (black line), significant isotherm at 500 hPa (dashed grey circle), maximum vorticity centre (grey crosses) and ridges (black zigzag).

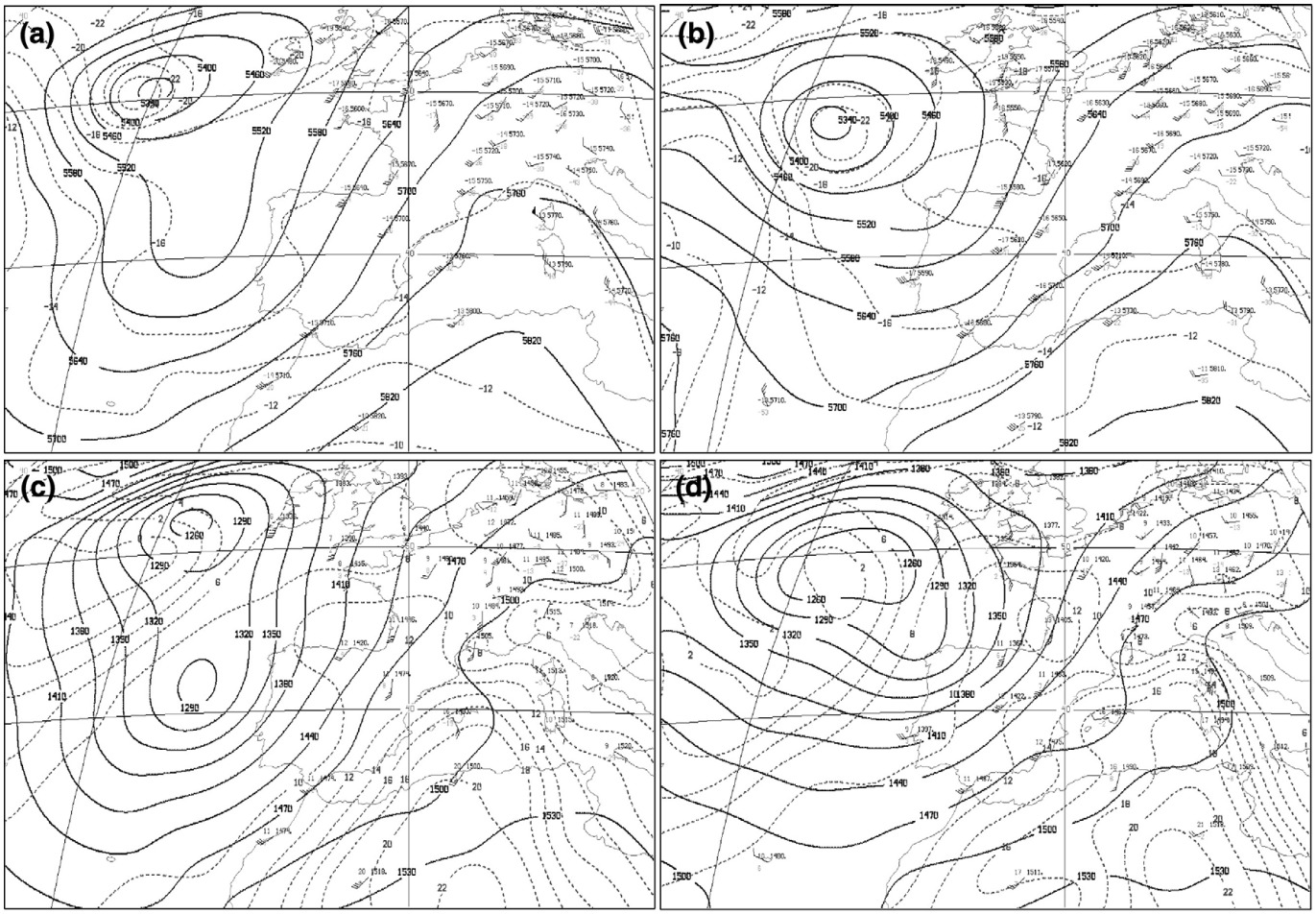

Fig. 3. Geopotential height (m, solid line) and temperature (°C, dashed line) from the objective analysis from ECWMF model: (a) 500 hPa at 00 UTC, (b) 500 hPa at 12 UTC, (c) 850 hPa at 00 UTC and (d) 850 hPa at 12 UTC.

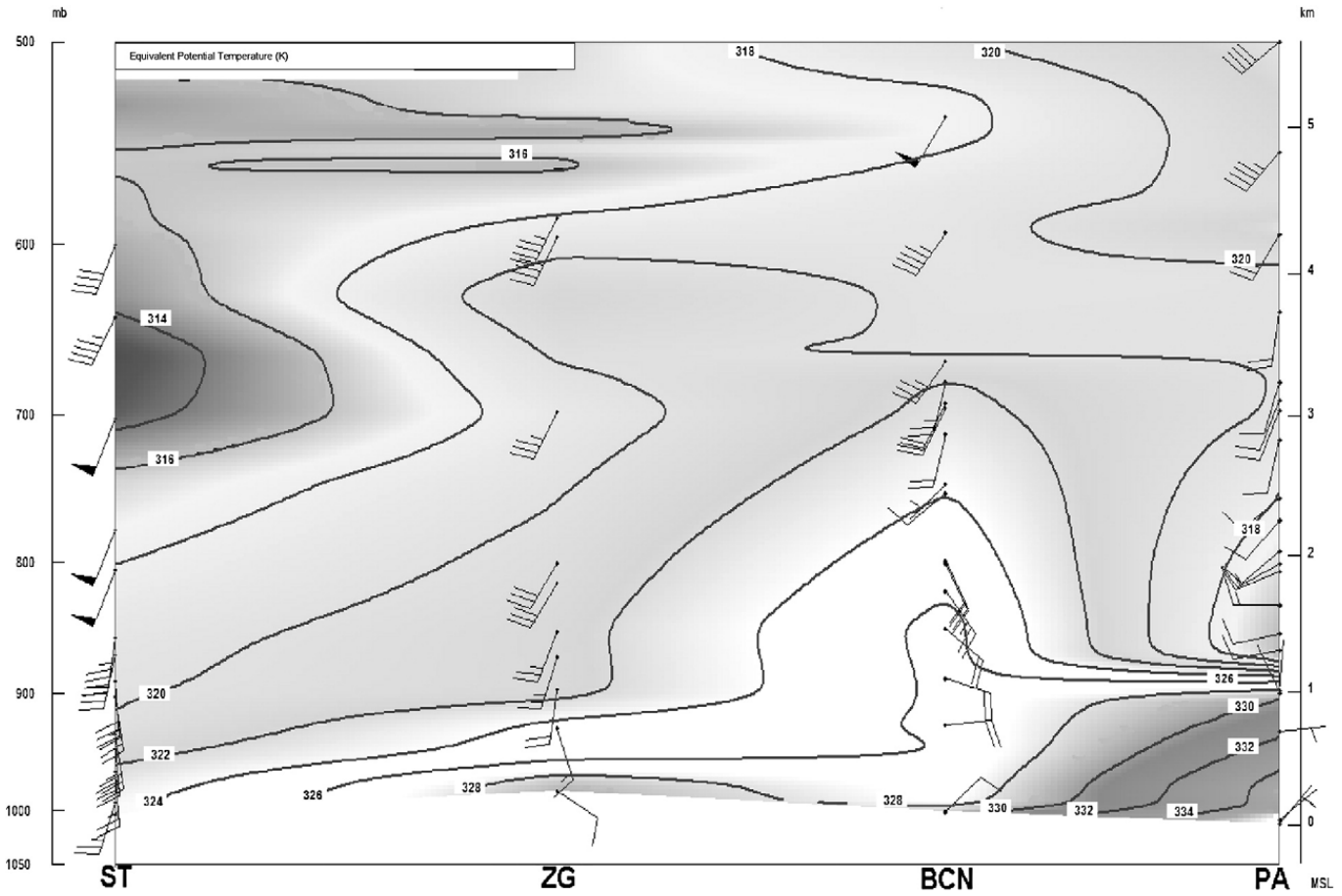

Fig. 4. Distance-based cross section using rawinsonde data of Santander (ST), Zaragoza (ZG), Barcelona (BCN) and Palma de Mallorca (PA) (see Fig. 1).

the anvil could have had greater influence. However, no AWS data allowed assessing cooling due to only the anvil effect; in some periods, cooling was also due to precipitation. Both mechanisms contributed to the generation of a thermal boundary in the area of study (Fig. 7c) more defined in the central and north coast. Furthermore, the strengthening of the easterly wind favoured the development of thermal ridges; the axis of one of them pointed to the area where the tornado took place.

3.2. Rawinsonde data

Rawinsonde data allow a detailed analysis of the main factors related with tornadogenesis: wind shear, low level moisture and convective energy available for the development of updrafts (Markowski and Straka, 2000; Markowski et al., 2002; Miller, 2006).

The closest rawinsonde to the studied area was launched in Barcelona, 45 km south from the tornado's location and approximately 90 min before the event. The rawinsonde release took place in the airmass that produced the tornado event. Therefore, the atmospheric profile obtained with these rawinsonde data can be considered representative of the mentioned area and for that period of time (Kerr and Darkow, 1996).

Following the criteria used by Whiteman et al. (1997) and Bonner (1968), an easterly low-level jet (LLJ) was located at 1740 m. The maximum speed was 12.4 m/s and decreased more than 6 m/s below 2800 m (Fig. 8). According to the study carried out by Toda et al. (2003) with rawinsonde data collected between 1997 and 2003 in Barcelona, these LLJs are not very frequent in this area, representing less than 8% of the cases.

The profile of the hodograph (Fig. 8) showed the presence of large bulk shear vectors at 12 UTC. In addition, the hodograph trace revealed a kink, characteristic of tornadic cases as other authors have found (Miller, 2006; Doswell, 1991). The storm relative helicity between 0–3 km was 267 m^2/s^2 and between 0–1 km was 141 m/s^2, which are significant values for tornadogenesis (Edwards and Thompson, 2000).

The easterly low-level jet favoured the advection of warm and moist air over the coastal zone. The lifting condensation level (LCL) and the level of free convection (LFC) were both low and equal: 428 m for parcel theory and 598 m using a mean layer of 100 hPa. It should be noted that the thermodynamic profile of the rawinsonde at 12 UTC could be contaminated by a light drizzle. Previously at 00 UTC (Fig. 9), the profile also presented an exceptionally humid airmass near surface but there was a very dry layer immediately above it. Mixing ratio was more than 12 g/Kg at both rawinsonde profiles but, at 00 UTC decreased with height roughly below 1800 m (not seen at 12 UTC because of the precipitation). In the layer below 1800 m, the temperature lapse rate was moderate (about −6 °C/km) which favoured instability.

Another factor for tornadogenesis is a persistent updraft. In this event, CAPE was not very high (see Table 1) but, as Gayà et al. (2001) pointed out, in the Balearic tornado events

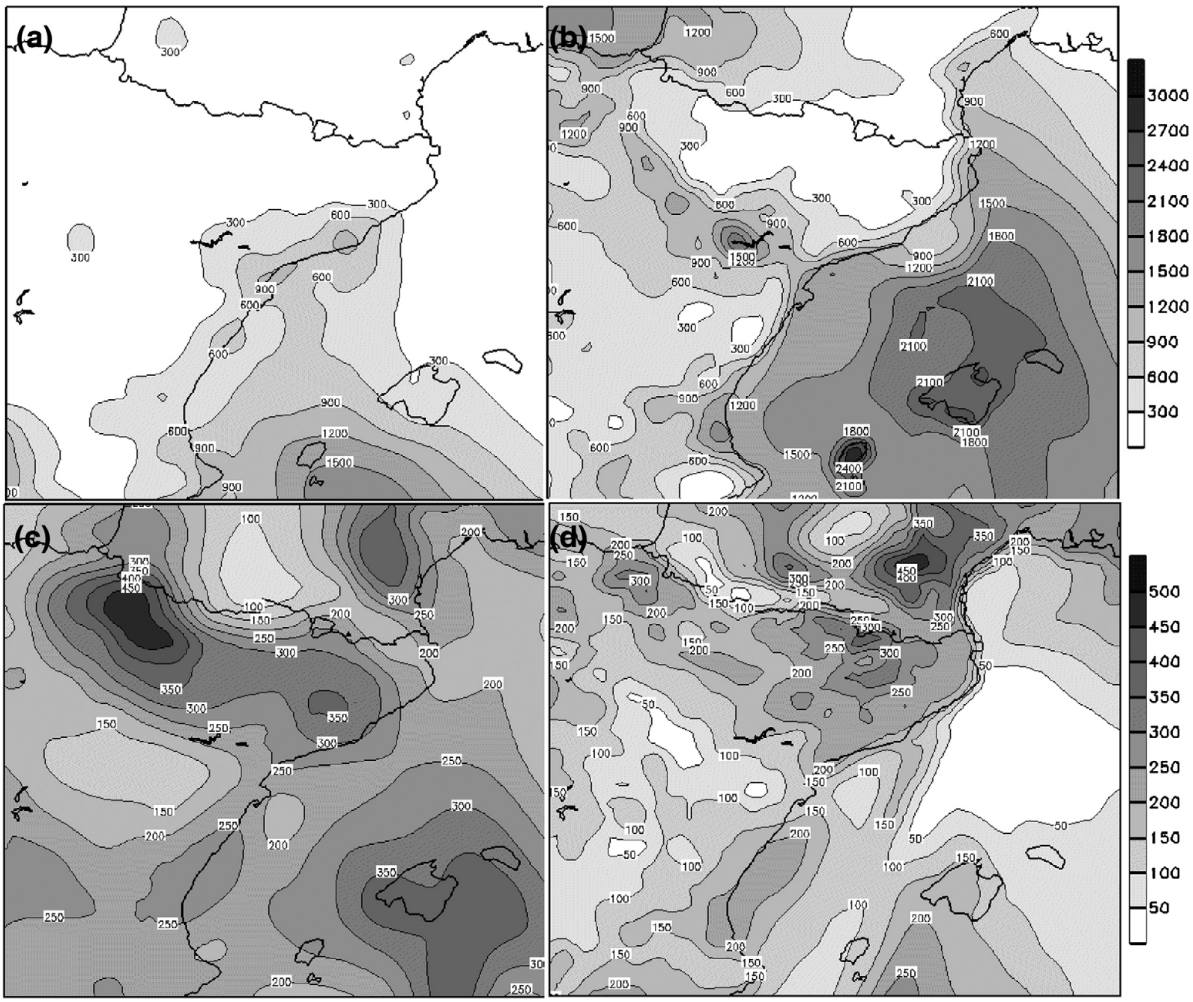

Fig. 5. Convective Available Potential Energy (J/kg) (a) at 00 UTC and (b) at 12 UTC. Storm Relative Helicity 0–3 km (m^2/s^2) analysis (c) at 00 UTC and (d) at 12 UTC.

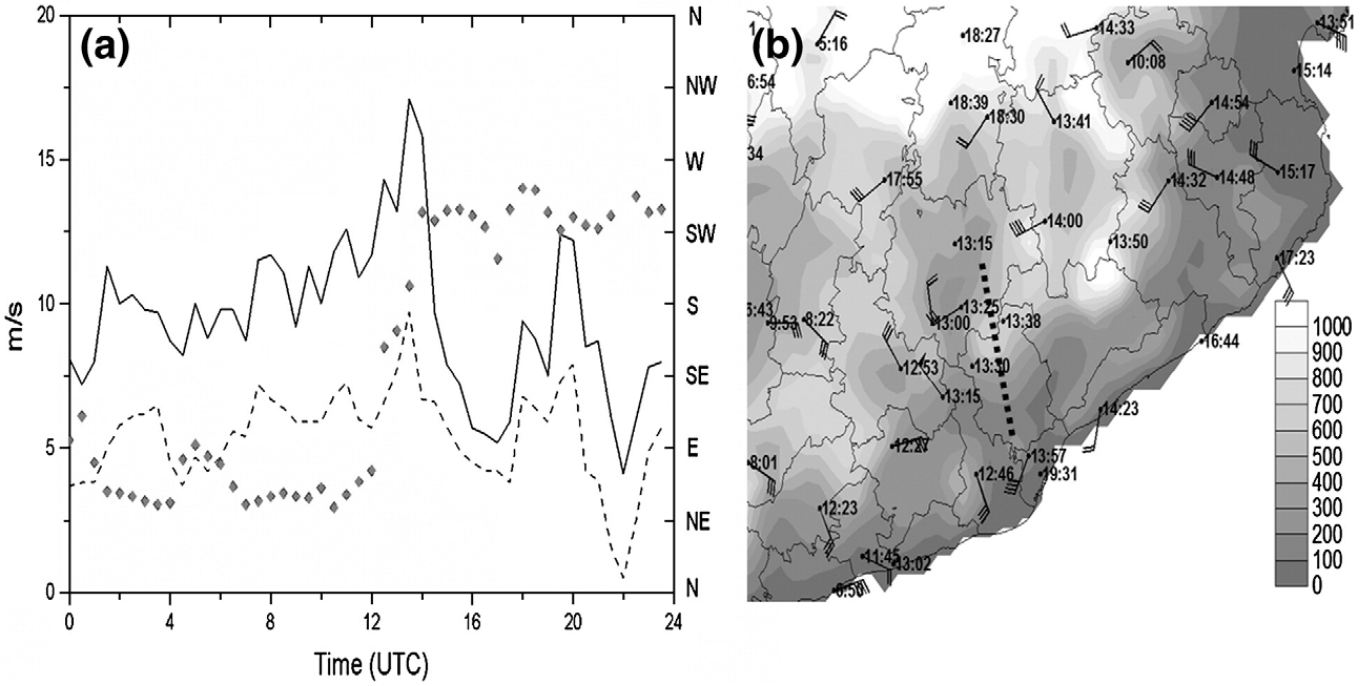

Fig. 6. (a) Wind of Barcelona Fabra Observatory Station: direction (diamonds), mean velocity (kts, dash black line) and gust velocity (kts, black line). (b) Barbs and hour of the strongest wind gust recorded by surface observations. Dashed black line corresponds to the convergence line near Castellcir.

these values were enough for developing tornadoes. A climatology of instability indices derived from ECMW ERA-40 analysis was described by Romero et al. (2007). In that study, instability indices associated to significant tornado events in Catalonia coincide with those obtained from Barcelona rawinsonde data (Table 1).

4. Mesoscale study

4.1. Satellite data

Fig. 10 corresponds to infrared images (channel 9, 10.8 μm) of MSG around the time of the tornado event in Castellcir and Fig. 11 to the microburst in Cabanes.

The main cluster of storms with temperatures lower than −52 °C reached a maximum area of 48.000 km2 at 16 UTC. According to Maddox's criteria (1980), this mesoscale structure does not correspond to a Mesoscale Convective Complex (MCC). The occurrence of this mesoscale phenomenon is very unlikely in the Iberian Peninsula. As reported by Riosalido et al. (1998a,b) in a study of MCCs in Spain, only 9% of the events accomplished Maddox definition and, as average, the area below that temperature was about 40.000 km^2. In the next section, using radar data, it will be defined as a Mesoscale Convective System (MCS) considering Houze's criteria (1993).

Using IR images the development of the MCS could be divided in 3 different stages. In the first one, between 12:30 and 13:15 UTC, new cells grew upwind. At 12:30 UTC, two clusters of storms started to merge. A second stage can be defined from 13:15 UTC to 15:15 UTC. It was just a few minutes before the tornado event when the storms merged and evolved to a MCS. In that system, the new cells grew downwind. In the last stage, from 15:15 UTC onwards, the MCS development was more intense (Fig. 12) and the new cells started again to grow upwind.

The analysis of the temporal evolution of −52 °C isotherm shows that the inflow flank of the system was quite stationary. Moreover, at upper levels, wind was not very strong so the MCS shape was rounded in concordance with the results of Heymsfield and Blackmer (1988).

4.2. Radar data

In this section radar reflectivity composite images recorded with the SMC C-band Doppler weather radar network (Bech et al., 2004) are examined. Complementary, wind profiles obtained from Velocity Volume Processing (VVP) products of the Barcelona radar are also used.

The composite images (Figs. 10 and 11) reveal the precipitation structure associated with the different stages described in the previous section with the MSG satellite data. During the initial stage (12:30 to 13:15 UTC), widespread and generally weak to moderate precipitation radar echoes were present in the western of Catalonia, moving from SW to NE. At the end of this initial stage, the structure was approximately elliptical, with the major axis exceeding 100 km, and thus satisfying the spatial criterion for a MCS (Houze, 1993). The overall picture of this MCS is similar to the broken areal squall line type, described by Bluestein and Jain (1985), evolving to an embedded areal type, i.e. with a line of more intense cores embedded in a larger stratiform region.

Later, in the second stage (13:15 to 15:15 UTC) this line of higher radar reflectivity intensified and expanded, as also did the stratiform part which was clearly located in the leading part of the system. These features are in good agreement with the leading stratiform squall line type described by Parker and Johnson (2000).

At the beginning of this stage, about 13:30 UTC, the Castellcir tornado took place. The cell that spawned the tornado did not exhibit particular characteristics in terms of intensity and

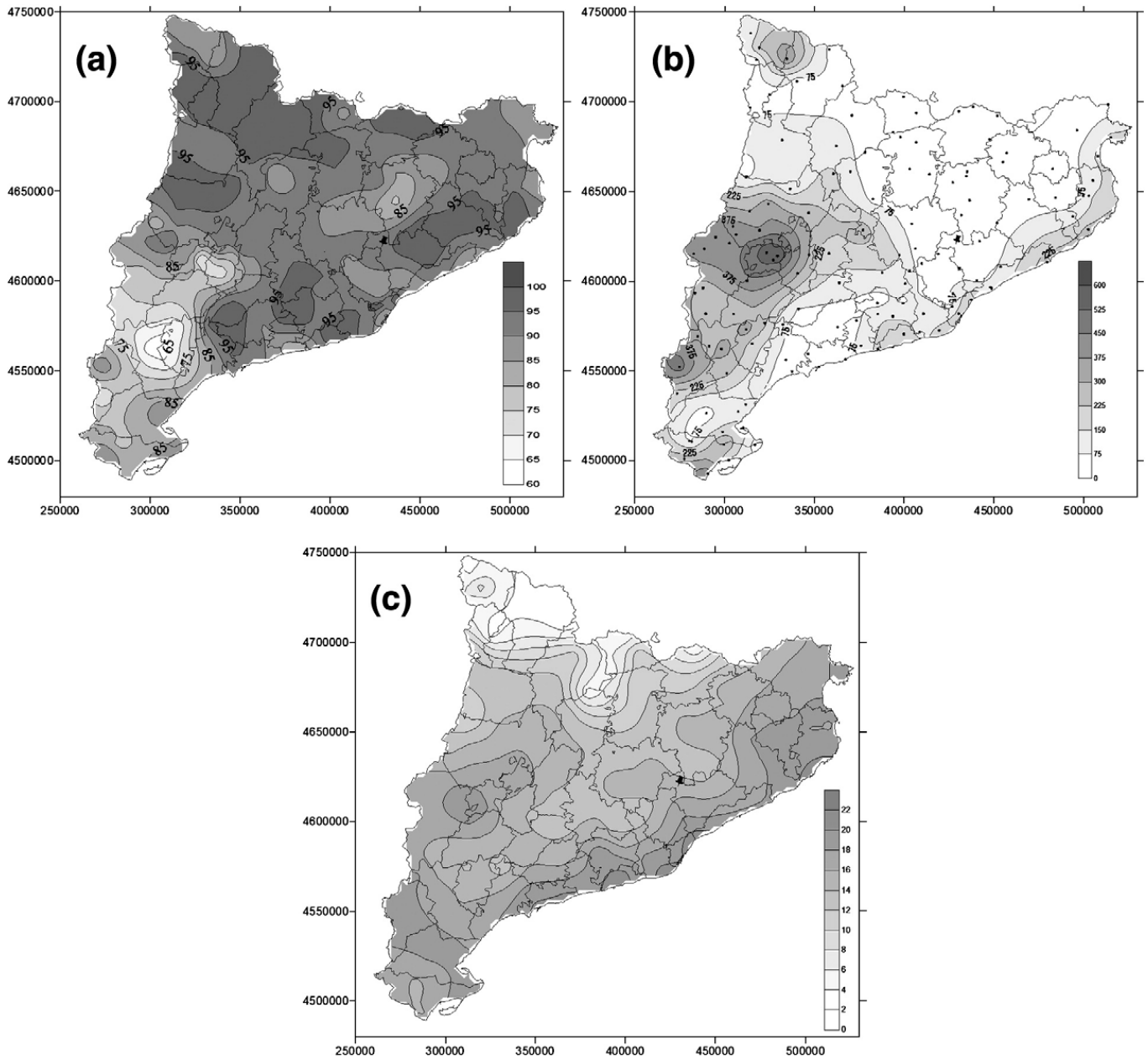

Fig. 7. Analysis of selected surface fields. (a) Mean relative humidity between 12 and 13 UTC. (b) Total solar radiation between 13 and 14 UTC and AWS locations (black points) used in the analysis. (c) Dew point (°C) at 13 UTC. The tornado position is also indicated (black mark).

height but this cell was included in a larger structure with an apparent comma shape. Behind this structure, a second one, larger and more intense, could have produced attenuation in the radar reflectivity field in that area. This hypothesis is consistent with images of the Agencia Estatal de Meteorología radar in Barcelona (not shown).

The Doppler radial-winds did not indicate clear signs of rotation revealing the presence of a rotating meso-cyclone and therefore, the supercell character of the tornado. However, it should be noted that the complex topography of this area produces beam blockage in the radar observations and this could degrade both the radial velocity and radar reflectivity patterns observed at low antenna elevation angles (Bech et al., 2003).

A very remarkable feature of the last part of the second stage is the arch shape of the most intense convective cores, a clear bow echo shape. This feature is a classical indicator of potential strong convective driven surface winds and therefore severe weather such as downbursts or tornadoes (Fujita, 1981; Przybylinski, 1995).

In the third stage, the bow echo split into two parts (Fig. 10, 15:24 UTC). Near the breaking point of the bow echo, in the municipality of Cabanes, a microburst was observed, i.e. damage was restricted to an area less than 4 km along a side.

Doppler radar observations helped to depict the role of wind shear in the evolution of the event using Velocity Volume Processing (VVP) images. Over the SMC Barcelona radar, the wind veered below 3 km (Fig. 13) from SE to SW and strengthened. A similar temporal evolution was observed in the other radars of the network.

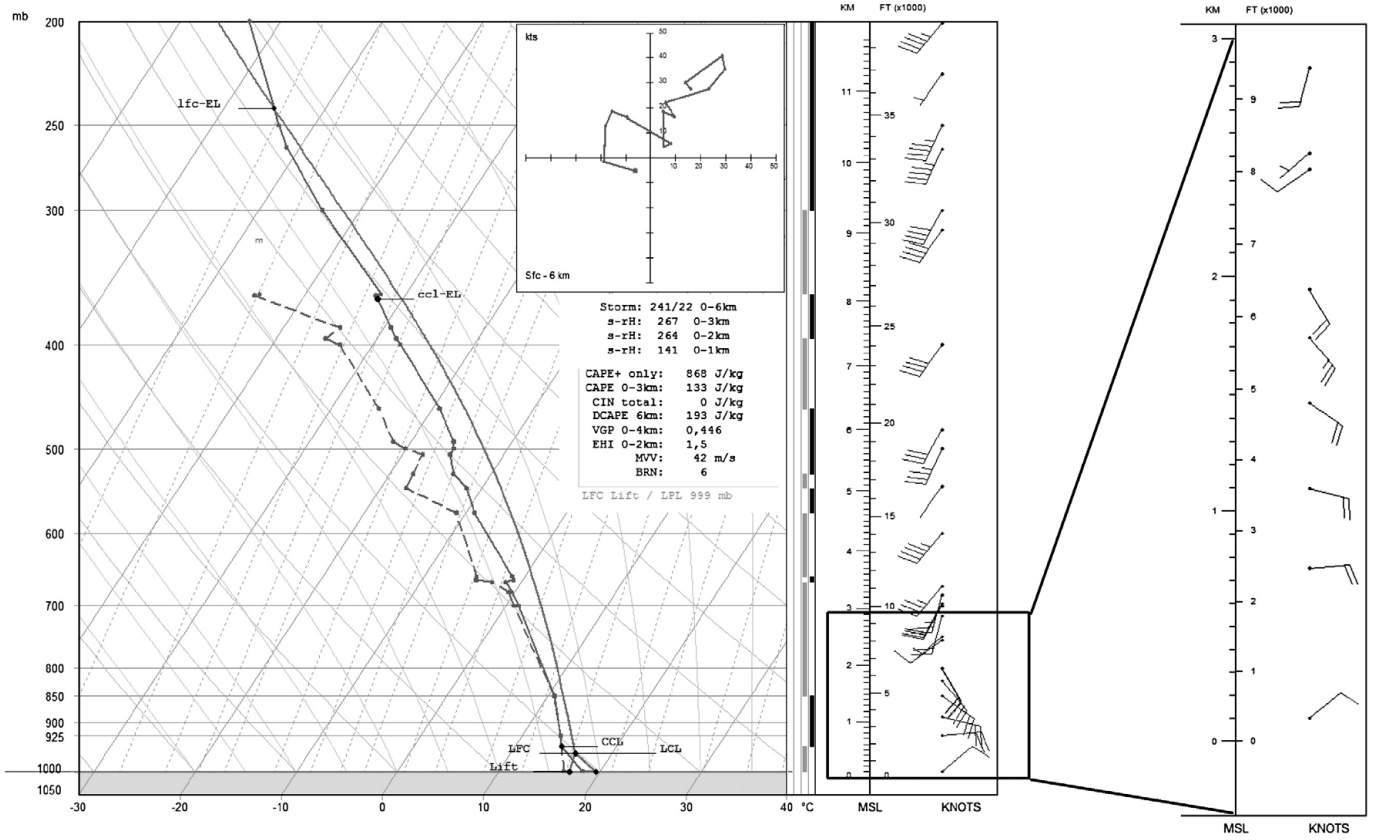

Fig. 8. Skew-T plots and hodograph at 18-10-2006 12 UTC in Barcelona. A zoom of the lowest part (0–3 km) of the wind profile is presented on the right.

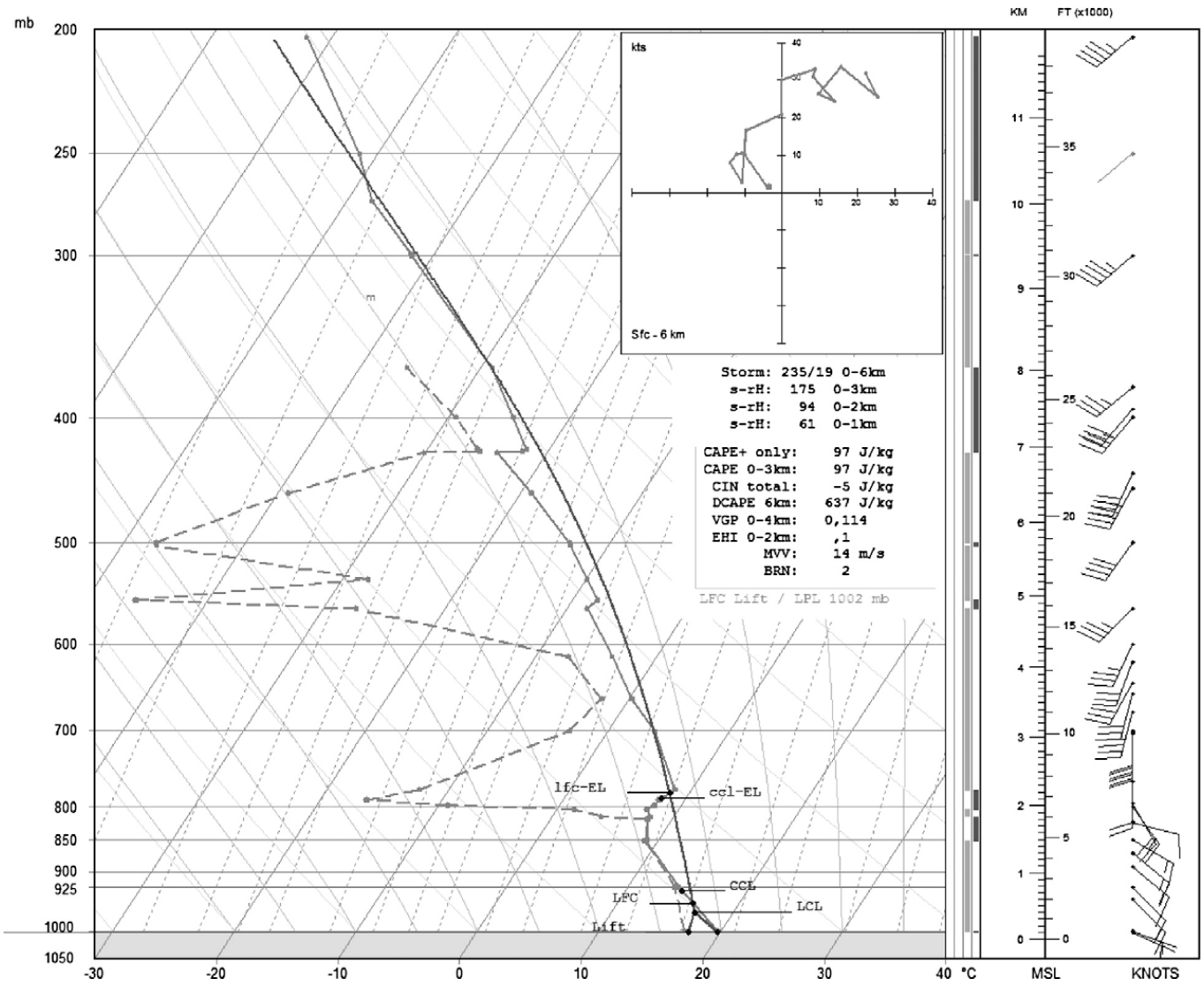

Fig. 9. As in Fig. 8 but for 18-10-2006 00 UTC in Barcelona.

4.3. Lightning data

The SMC operates a SAFIR lightning detection system. It uses an interferometric technique in the VHF range (108–116 MHz) to detect total lightning flashes (Richard and Lojou, 1996). The SAFIR system discriminates intra-cloud (hereafter IC) flashes and cloud-to-ground (hereafter CG) flashes.

Lightning flashes of the thunderstorm associated with the tornado have been examined. The cell's perimeter of the thunderstorm was delimited using 15 dBZ isolines in radar reflectivity images. Fig. 14 shows the time series of the flashes considered between 12 and 14 UTC. Because of the number of CG flashes was low, this analysis focused on the temporal evolution of the rate of +CG versus CG and the IC flashes.

Two different stages can be defined in the evolution of the thunderstorm of interest. These stages coincide with the two first periods described in the analysis of IR images. Before 12:30 UTC, no flashes were registered within the perimeter of the storm. The first stage was between 12:30 and 13:15 UTC. At 12:30 UTC, the storm began to produce incipient lightning. There were 39 IC flashes and 24 CG flashes, 62% +CG and 38% −CG respectively. The percentage of +CG versus CG was anomalously high, more than 25%. Other studies indicate that this feature is associated to severe weather (see for example Carey et al., 2003). The number of IC was very low the whole period.

In the second stage, 13:15 to 15 UTC, IC flashes increased dramatically from 39 to 793. However, just before the onset of the tornado CG flashes decreased as other authors found in non-supercellular tornado events (Martin et al., 1997; Bechini et al., 2001). It is also remarkable an abrupt increase of total lightning (IC and CG) flash rate about 15 min prior to the tornado. In some studies this feature, known as lightning

Table 1

	CAPE (J/kg)	LR7050 (°C/km)	PRW85 (mm)
18 October 2006 00 UTC	97	4.8	19
18 October 2006 12 UTC	868	6.3	16
October 12 UTC (ERA-40 climatology)	100–200	6.4–6.6	13–14

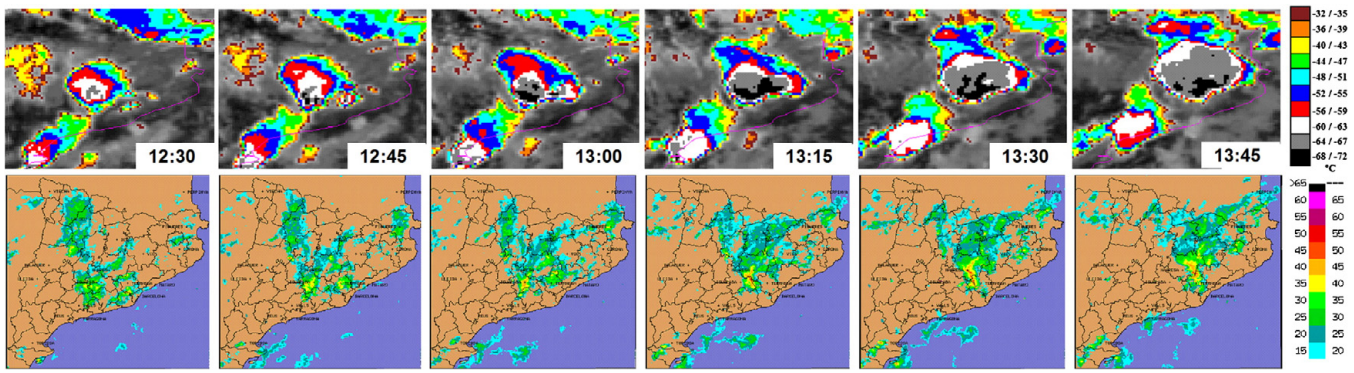

Fig. 10. Images of IR channel of the MSG (top) and base level PPI composite images of radar network of SMC (bottom). The tornado event was at 13:30 UTC.

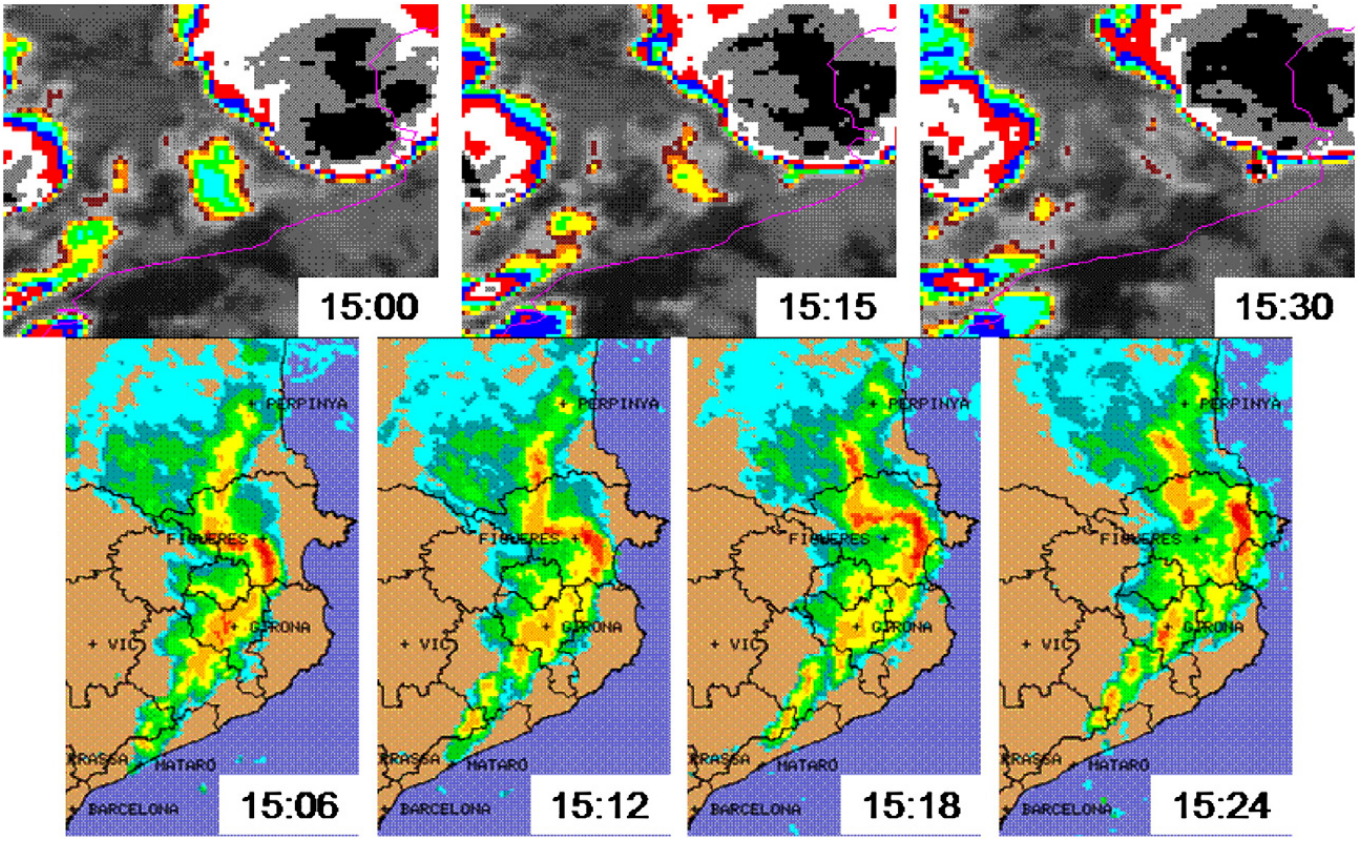

Fig. 11. Same as in Fig. 10. The Cabanes microburst was by 15:20 UTC.

jump, has been suggested as a precursor to severe weather (Williams et al., 1999).

5. Conclusions

A synoptic and mesoscale analysis of a tornadic event in Castellcir, Spain (18th October, 2006) has been presented. There were witnesses very close to the path of the tornado which caused F2 damage but, fortunately, there were no injuries.

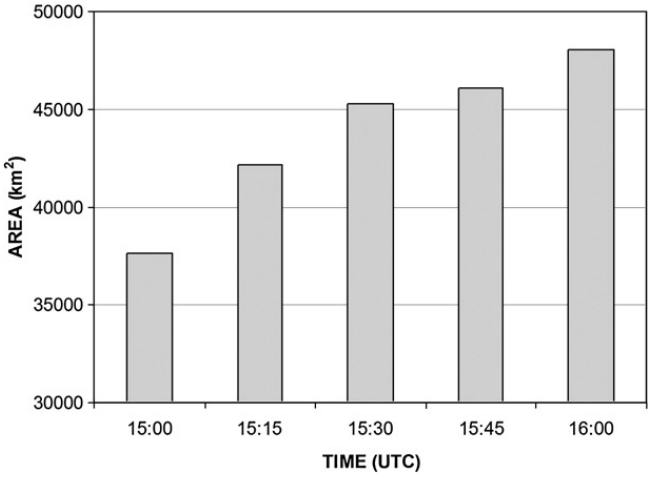

Fig. 12. Area of IR temperature below −52 °C (in km^2).

Although no strong forcing for upward vertical motion can be identified from the synoptic analysis, conditions were suitable for the development of convection. Furthermore, the synoptic environment was similar to other tornado events reported in the Western Mediterranean area.

On the other hand, rawinsonde data provided useful information about wind shear, absolute moisture and instability indices of the airmass close to the area of study. The presence of an easterly low level jet and the profile of the hodograph are characteristic of tornadogenesis. Despite the CAPE value was not very high the level of free convection was low enough to favour the vertical development. As a result, it is concluded that in this event triggering mechanisms did not play a crucial role.

A thermal boundary was detected using surface observations. Different factors could have contributed to the origin of this boundary like a warm air advection from maritime easterly winds, the cooling effect due to the precipitation and the differential cooling due to cloud cover.

Operational radar observations provided details of the system structure. They allowed defining it as a mesoscale convective system and no clear meso-cyclone was found linked to supercell features. Moreover, at the last stage of the MCS a bow echo which caused a microburst was detected at the northeast of Catalonia.

The analysis of intra-cloud and cloud-to-ground flashes suggests three stages of the MCS. Interestingly, similar results are obtained from the IR images study. It is also remarkable the detection of an abrupt increase of total lightning,

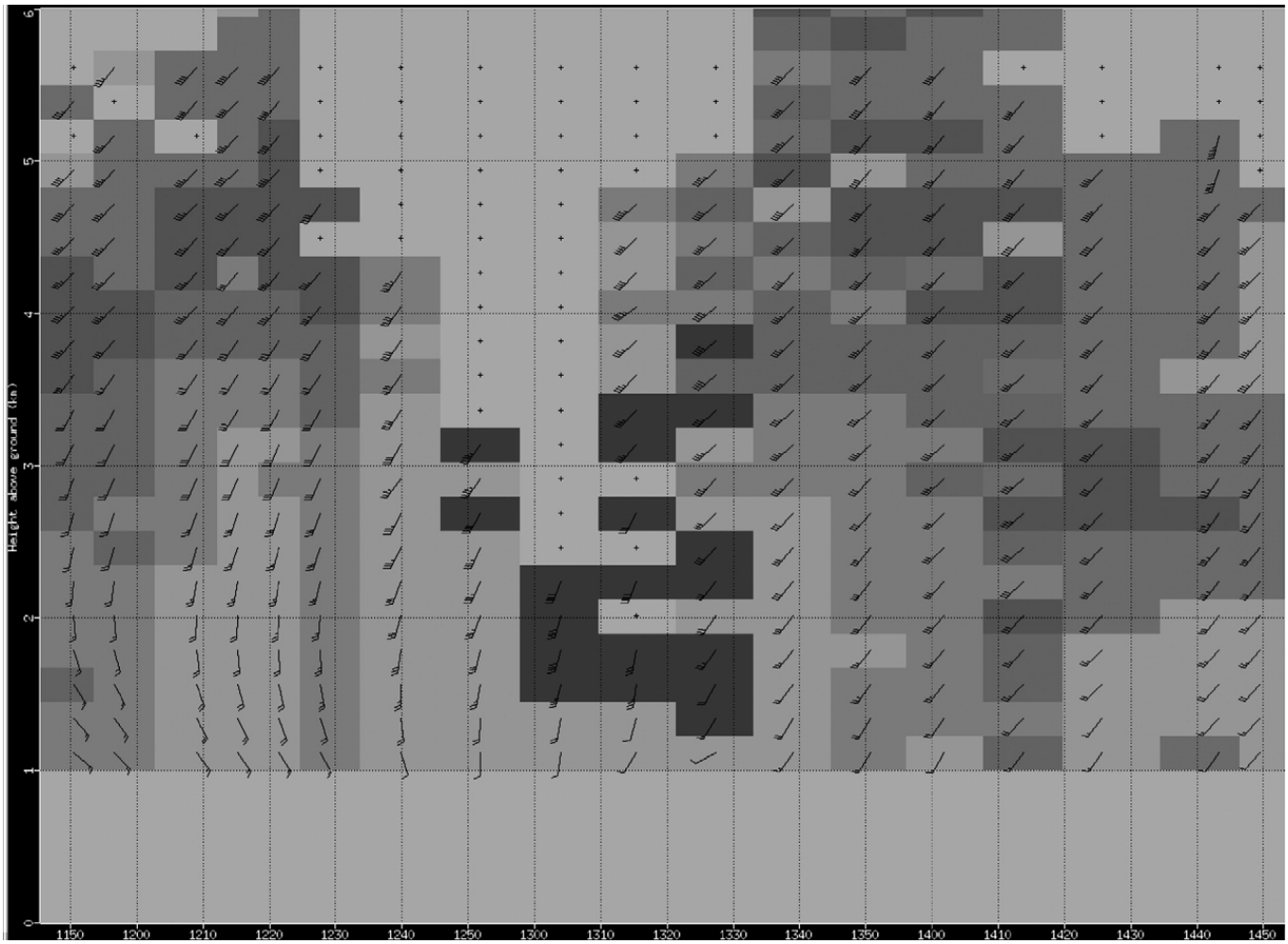

Fig. 13. Temporal evolution of the Velocity Volume Processing radar wind profile recorded by SMC Barcelona weather radar.

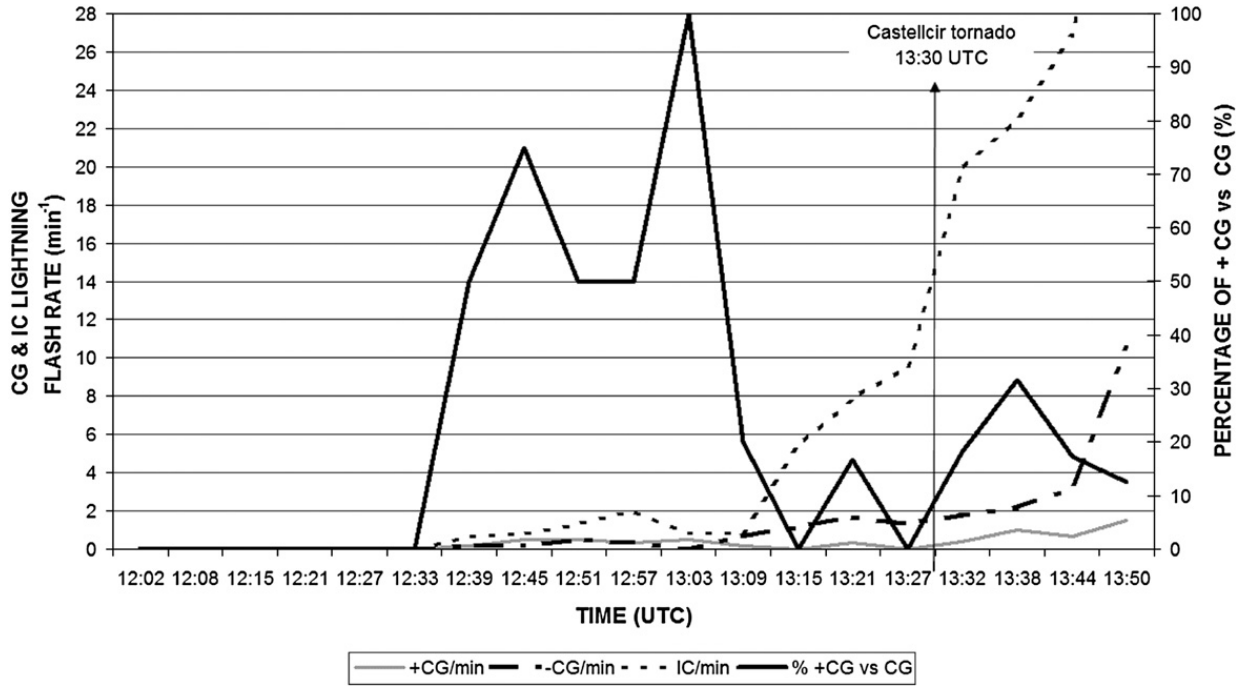

Fig. 14. Temporal evolution of lightning.

especially intra-cloud flashes, about 15 min prior to the tornado.

Acknowledgments

The authors would like to thank: J. Campins and A. Genovés of the Agencia Estatal de Meteorogía in the Balearic Islands; J. Moré, M. Bravo, N. Pineda, L. Trapero and T. Rigo of the SMC; R. Romero of the Universitat de les Illes Balears, and Marta Aran for their help and encouragement in this study. This study was done under the framework of the Cooperation Agreement (2002) between the Agencia Estatal de Meteorología of Spain and the Environment Department which hosts the Meteorological Service of Catalonia.

References

Barrera, A., Llasat, M.C., Barriendos, M., 2006. Estimation of extreme flash flood evolution in Barcelona County from 1351 to 2005. Nat. Hazards Earth Syst. Sci. 6, 505–518.

Bech, J., Codina, B., Lorente, J., Bebbington, D., 2003. The sensitivity of single polarization weather radar beam blockage correction to variability in the vertical refractivity gradient. J. Atmos. Oceanic Technol. 20, 845–855.

Bech, J., Rigo, T., Pineda, N., Segalà, S., Vilaclara, E., Sánchez-Diezma, R., Sempere-Torres, D., 2004. Implementation of the EHIMI Software Package in the Weather Radar Operational Chain of the Catalan Meteorological Service. 32nd Conf. on Radar Meteorology. American Meteorological Society.

Bech, J., Pascual, R., Rigo, T., Pineda, N., López, J.M., Arús, J., Gayà, M., 2007a. An observational study of the 7 September 2005 Barcelona tornado outbreak. Nat. Hazards Earth Syst. Sci. 7, 129–139.

Bech, J., Gayà, M., Aran, M., Figuerola, F., Amaro, J., Arus, J., 2007b: Tornado Damage Analysis of a Forest Area Using Site Survey Observations, Radar Data, and a Simple Analytical Vortex Model. (This voume).

Bechini, R., Giaiotti, D., Manzato, A., Stel, F., Micheletti, S., 2001. The June 4th 1999 severe weather episode in San Quirino, Italy: a tornado event? Atmos. Res. 56, 213–232.

Bluestein, H.B., Jain, M.H., 1985. Formation of mesoscale lines of pirecipitation: severe squall lines in Oklahoma during the spring. J. Atmos. Sci. 42, 1711–1732.

Bonner, W.D., 1968. Climatology of the low-level jet. Mon. Weather Rev. 96, 833–850.

Campins, J., Aran, M., Genovés, A., Jansà, A., 2007. High impact weather and cyclones simultaneity in Catalonia. Adv. Geosci. 12, 115–120.

Carey, et al., 2003. Evolution of cloud-to-ground lightning and storm structure in the Spencer, South Dakota, Tornadic Supercell of 30 May 1998. Mon. Weather Rev. 131, 1811–1831.

Davies, J.M., Johns, R.H., 1993: Some Wind and Instability Parameters Associated with Strong and Violent Tornadoes. Part 1. Wind Shear and Helicity. The Tornado: Its Structure, Dynamics, Prediction, and Hazards, Geophys. Monogr., No. 79, Amer. Geophys. Union, 573–582.

Doswell, C.A., 1991. A review for forecasters on the application of hodographs to forecasting severe thunderstorms. Natl. Weather Dig. 16 (No. 1), 2–16 Available at http://www.nssl.noaa.gov/~doswell/hodographs/hodographs.html.

Edwards, R., Thompson, R.L., 2000. RUC-2 supercell proximity soundings, Part II: an independent assessment of supercell forecast parameters. Preprints, 20th AMS Conference on Severe Local Storms, Orlando.

Fujita, T.T., 1981. Tornadoes and downbursts in the context of generalized planetary scales. J. Atmos. Sci. 38, 1511–1534.

Gayà, M., 2005. Tornadoes in Spain (1987–2005): Temporal and Spatial Distribution (in Spanish). Rev. Climatol. 5, 9–17 http://webs.ono.com/usr012/reclim/reclim05b.pdf.

Gayà, M., Homar, V., Romero, R., 2001. Tornadoes and waterspouts in the Balearic Islands phenomena and environment characterization. Atmos. Res. 56, 253–267.

Heymsfield, G.M., Blackmer Jr., R.H., 1988. Satellite-observed characteristics of Midwest severe thunderstorm anvils. Mon. Weather. Rev. 116, 2200–2224.

Homar, V., Gayà, M., Ramis, C., 2001. A synoptic and mesoscale diagnosis of a tornado outbreak in the Balearic Islands. Atmos. Res. 56, 31–55.

Homar, V., Gayà, M., Romero, R., Ramis, C., Alonso, S., 2003. Tornadoes over complex terrrain: an analysis of the 28th August 1999 tornadic event in eastern Spain. Atmos. Res. 67–68, 301–318.

Houze, R., 1993. Cloud Dynamics. International Geophysics Series, vol. 53. Academic Press.

Kerr, B.W., Darkow, G.L., 1996. Storm-relative winds and helicity in the tornadic thunderstorm environment. Weather Forecast. 11, 489–505.

Maddox, R., 1980. Mesoscale convective complexes. Bull. Amer. Meteor. Soc. 61, 1374–1387.

Markowski, P.M., Straka, J.M., 2000. Some observations of rotating updrafts in low-buoyancy, highly-sheared environments. Mon. Weather Rev. 128, 449–461.

Markowski, P.M., Rasmussen, E.N., Straka, J.M., Dowell, D.C., 1998. Observations of low-level baroclinity generated by anvil shadows. Mon. Weather Rev. 126, 2942–2958.

Markowski, P.M., Straka, J.M., Rasmussen, E.N., 2002. Direct surface thermodynamic observations within the rear-flank downdrafts of nontornadic and tornadic supercells. Mon. Weather Rev. 130, 1692–1721.

Martín, F., Riosalido, R., de Estevan, L., 1997. The Sigüenza tornado: a case study based on convective ingredients concept and conceptual models. Met. Appl. 4, 191–206.

Mateo, J., Ballart, D., Brucet, C., Aran, M., Bech, J., 2009. A study of a heavy rainfall event and a tornado outbreak during the passage of a squall line over Catalonia. Atmos. Res. 93, 131–146 (this issue).

Miller, D.J., 2006. Observations of low level thermodynamic and wind shear profiles on significant tornado days. Preprints, 23rd Conference on Severe Local Storms. St. Louis.

Parker, M.D., Johnson, R.H., 2000. Organizational modes of midlatitude mesoscale convective systems. Mon. Weather Rev. 128, 3413–3436.

Pascual, R., Callado, A., 2002. Mesoanalysis of recurrent convergence zones in the north-eastern Iberian Peninsula. Proceedings of the ERAD-2002, pp. 59–64.

Przybylinski, R.W., 1995. The Bow Echo: observations, numerical simulations, and severe weather detection methods. Weather Forecast. 10, 203–218.

Richard, P., Lojou, J.Y., 1996. Assessment of application of storm cell electrical activity monitoring to intense precipitation forecast. In 10th Int. Conf. on Atmospheric Electricity, Osaka, Japan, pp. 284–287.

Riosalido, R., Rivera, A., Martin, F., 1998. Development of a mesoscale convective system in the Spanish Mediterranean Area. Proc. 7th Meteosat Scientific Users' Meeting. Madrid, EUM P 04, pp. 375–378. 27–30, Sept.

Romero, R., Gayà, M., Doswell, C.A., 2007. European climatology of severe convective storm environmental parameters: a test for significant tornado events. Atmos. Res. 83, 389–404.

Toda, J., Aran, M., Moré, J., Sairouni, A., Miró, J.R., 2003. Towards a Rawindsonde Data Base. First Results. 5th Plinius Conference on Mediterranean Storms, Ajaccio.

Whiteman, C.D., Bian, X., Shiyuan, Zhong., 1997. Low-level jet climatology from enhanced rawinsonde observations at a site in the Southern Great Plains. J. Appl. Meteor. 36, 1363–1376.

Williams, et al., 1999. The behaviour of total lightning activity in severe Florida thunderstorms. Atmos. Res. 51, 245–265.